

## Thermodynamic model for predicting hydrogen segregation at grain boundaries for bcc-iron

Sojeong Yang, Takuji Oda\*

Department of Nuclear Engineering, Seoul National University, 1 Gwanak-ro, Gwanak-gu, Seoul, Republic of Korea

\*Corresponding author: oda.snu.ac.kr

### 1. Introduction

Hydrogen embrittlement is one of the significant issues in maintaining the integrity of structural components in nuclear reactors because hydrogen is inevitably generated from fabrication or corrosion as well as by some nuclear reactions in nuclear materials, and hydrogen isotopes are the fuel for the fusion reactor. In many structural materials including stainless steels, the hydrogen behavior is known to be highly influenced by defects. Among several typical lattice defects, grain boundaries (GBs) are important because hydrogen is easily trapped at GBs and consequently lowers the cohesion energy. However, due to the complexity and diversity of GBs, predicting hydrogen behaviors, such as solubility and diffusivity, has limits in the accuracy unlike for the case of perfect crystals.

In our previous study, by using molecular dynamics (MD) simulation, the solubility and diffusivity of hydrogen in a GB-incorporated bcc-iron, which is a base metal for many structural components, were determined for a specific GB ( $\Sigma 19b, \langle 111 \rangle 46.8^\circ, \{5-3-2\}$ ) as a function of the hydrogen concentration [1]. However, it is practically difficult to perform MD simulations for many different types of GBs in diverse conditions, such as different external hydrogen pressure, grain size, and temperatures. Therefore, in this study, we aim to construct thermodynamic models that can predict the segregation of hydrogen to a GB, focusing on the bcc-iron. The performance of the models are verified by the comparison with MD simulation results.

### 2. Methods

#### 2.1. Grain boundary structure and characteristics

We investigated bcc-iron bicrystal systems containing  $\Sigma 5[001](310)$  GB, which has a  $[001]$  tilt axis and  $(310)$  GB plane. The structure of the GB is presented in Fig. 1. The system dimension after the geometry optimization at 0 K was  $27.00 \text{ \AA} \times 28.48 \text{ \AA} \times 54.96 \text{ \AA}$  with 3600 Fe atoms. The interstitial sites for H atoms at around the GB were searched by inserting a hydrogen into a grid of  $0.5 \text{ \AA}$  intervals for each axis, and then optimizing the structure with fixed 0 K equilibrium volume. Considering the effect of thermal expansion, the binding energy of hydrogen trapped at GB per H atom in the equilibrium volume for temperature  $T$  ( $e_b(T)$ ) was calculated as

$$e_b(T) = \left\{ E_{GB}(T) + E_{bulk,H}(T) \right\} - \left\{ E_{GB,H}(T) + E_{bulk}(T) \right\}, \quad (1)$$

where  $E_{GB}(T)$  is the energy of the system containing the GB,  $E_{bulk,H}(T)$  is the energy of a perfect bcc-iron crystal system with one hydrogen located at tetrahedral site sufficiently away from the GB,  $E_{GB,H}(T)$  is the energy of the system containing hydrogen trapped at the GB, and  $E_{bulk}(T)$  is the energy of the perfect bcc-iron crystal system. All these values were obtained at the equilibrium volume of temperature  $T$  to take into account the effect of thermal expansion of the bcc lattice. The binding energy of hydrogen at interstitial sites around the GB at the equilibrium volume of 600 K is shown in Fig. 2. Each interstitial site is numbered from site-1 to site-9 in order of distance from the GB center, and we refer the tetrahedral site in bulk as site-10. In MD results, it was difficult to distinguish between hydrogen lying on closely located interstitial sites, such as between site-1, site-2 and site-3, because of the atomic vibration. Therefore, we used 5 regions, from  $A_1$  (closest region to the GB center) to  $A_5$  (bulk region) as shown in Fig. 2, to compare the equilibrium fraction of hydrogen with MD results.

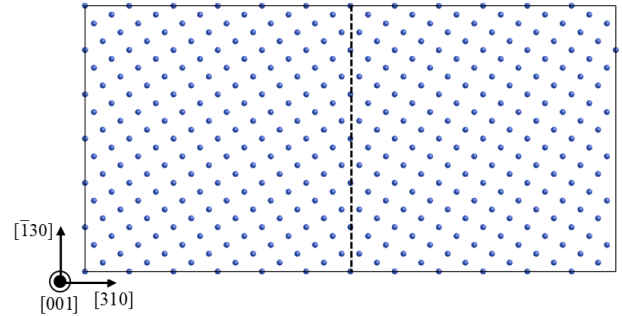


Fig. 1. The optimized structure of  $\Sigma 5[001](310)$  GB at 0 K.

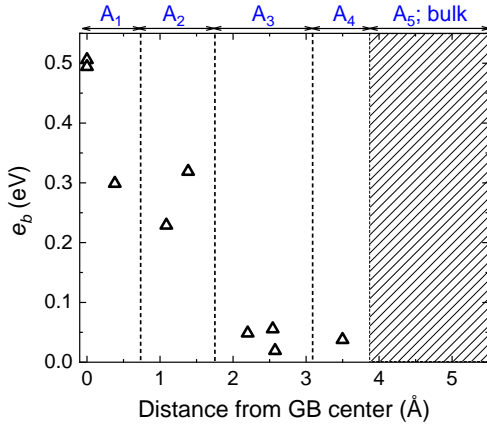


Fig. 2. The binding energy of hydrogen per atom at interstitial sites around GB at the equilibrium volume of 600 K as a function of the distance from GB center.

## 2.2. Thermodynamic model with configurational entropy (model-1)

To predict the segregation of hydrogen at GB, we constructed a thermodynamic model using equilibrium theory. First, we applied a simple model assuming that the contribution of vibrational entropy is negligible but the contribution of configurational entropy is high. Then, the Helmholtz free energy  $A$  is expressed as

$$A = E - TS = -N_H \sum_i (f_i e_{b,i}) - kT \ln W, \quad (2)$$

$$\ln W = \sum_{i=1}^{10} \ln \binom{n_i}{N_H f_i} \quad (3)$$

$$\sim \sum_{i=1}^{10} \left( n_i \ln n_i - f_i N_H \ln f_i N_H - (n_i - f_i N_H) \ln (n_i - f_i N_H) \right),$$

$$\sum_{i=1}^{10} f_i = 1, \quad (4)$$

where  $N_H$  is the number of hydrogen in the MD system, which is 10 and 160 in this study,  $f_i$  is the hydrogen fraction at site  $i$ ,  $e_{b,i}$  is the binding energy of hydrogen per atom at site  $i$ ,  $k$  is the Boltzmann constant, and  $W$  is the number of possible configurations. When  $n_i$  is the number of available sites for H atom and  $N_H f_i$  is the number of H atoms at an equilibrium state at site  $i$ , the number of possible configurations in the system is the multiplication of the possible configuration for each site, which is  $\binom{n_i}{N_H f_i}$ . The  $n_i$  values in the current supercell are presented in Table 1. Then, using Starling's approximation,  $\ln W$  term can be expanded as presented in Eq. (3). In addition, the summation of the hydrogen fraction should be 1 as presented in Eq. (4). The equilibrium fraction of hydrogen at each interstitial site was calculated by minimizing the Helmholtz free energy  $A$  with respect to  $f_1, f_2, \dots$ , and  $f_{10}$ , which is achieved by

$$\frac{\partial A}{\partial f_1} = \dots = \frac{\partial A}{\partial f_{10}} = 0. \quad (5)$$

Table 1. The number of available sites for H atom at each site; from  $n_1$  to  $n_{10}$ .

$n_1$	$n_2$	$n_3$	$n_4$	$n_5$
120	120	240	240	240
$n_6$	$n_7$	$n_8$	$n_9$	$n_{10}$
240	240	240	240	19600

## 2.3. Thermodynamic model with vibrational entropy in addition (model-2)

In model-2, not only the configurational entropy but also the vibrational entropy contributes to the Helmholtz energy, which is expressed as

$$A = E - T(S_{conf} + S_{vib}) \quad (6)$$

$$= -N_H \sum_i (f_i e_{b,i}) - kT \ln W - TN_H \sum_i (f_i s_i),$$

where  $S_{vib}$  is the vibrational entropy, and  $s_i$  is the vibrational entropy difference per H atom from site  $i$  with site 10 (bulk), which is used as the reference site. The vibrational entropy at each site was calculated by lattice dynamics under harmonic approximation [2]. Then, the equilibrium fraction of hydrogen at each interstitial site was calculated with the same procedure described in model-1.

## 2.4. Computational details for molecular dynamics simulation

Classical molecular dynamics simulations were performed by using Large-Scale Atomic/Molecular Massively Parallel Simulator (LAMMPS) [3] to validate our thermodynamic models. Systems with bcc iron and hydrogen were modelled by an embedded atom method (EAM) potential parameterized by Ramasubramaniam et al. [4]. In order to obtain the segregated fraction of hydrogen at the GB, GB systems with randomly inserted hydrogen of 10 or 160 H atoms were first equilibrated with NPT ensemble for 0.4 ns and then the production run was conducted with NVT ensemble for 30 ns at 600 K.

## 3. Results and Discussions

The equilibrium fractions of hydrogen in the systems with the GB were obtained at 600 K by the MD simulation and by the thermodynamic models, which are compared in Fig. 3. In the case of the system with 10 H atoms ( $\text{Fe}_{3600}\text{H}_{10}$ ), the model-2, which also includes vibrational entropy effects, performed better in reproducing MD results. In contrast, for the system with 160 H atoms, both models overestimated the hydrogen fraction at the GB, particularly at the  $A_1$  region, which is due to the interaction between H atoms. In Fig. 2, the

$e_b$  was calculated in the system with only one H atom. However, as the hydrogen concentration increases, H atoms can be located at the nearest interstitial sites around the GB and then the interaction between trapped H atoms changes  $e_b$  values. Yamaguchi et al. [5] observed a decrease in  $e_b$  value with increasing the hydrogen concentration in bcc iron for  $\Sigma 3(111)$  GB by first-principles calculations. This result implies that the binding energy of H atoms to the GB decreases due to the interaction between trapped H atoms, resulting in a lower fraction of hydrogen at GB than the fraction calculated on the assumption of non-interacting H atoms. For a better performance of the models, the quantitative analysis for the interaction between hydrogen is needed, which will be discussed in the presentation.

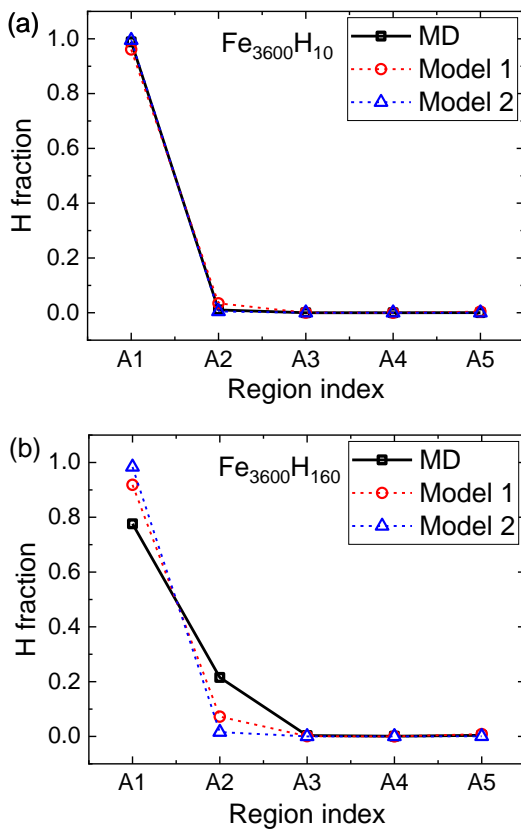


Fig. 3. The equilibrium fractions of hydrogen resulted from MD simulation, and thermodynamic models constructed in this study, with the systems of bcc iron  $\Sigma 5[001](310)$  GB at 600 K; (a)  $\text{Fe}_{3600}\text{H}_{10}$ , (b)  $\text{Fe}_{3600}\text{H}_{160}$ .

#### 4. Conclusion

The segregation of hydrogen at GB interstitial sites and in bulk sites were predicted using two thermodynamic models based on the equilibrium theory. The first model considered only configurational entropy in the free energy, while in the second model, not only configurational entropy but also vibrational entropy contributed to the free energy calculation. For the verification of the results obtained by the models, MD

simulation was used. At a low hydrogen concentration, the model that did not neglect the vibrational entropy in free energy calculation showed better performance. However, at a high hydrogen concentration, both the model considering only the configurational entropy and the model considering the vibrational entropy overestimate the equilibrium fraction of hydrogen at the GB because of the interaction between hydrogen. By including the effect of hydrogen interaction, we expect that the model can accurately predict the segregated fraction of hydrogen at the GB even at high concentrations of hydrogen, which will be discussed in the presentation.

#### 5. Acknowledgement

This work was supported by the R&D Program through the National Fusion Research Institute (NFRI) funded by the Ministry of Science and ICT of Republic of Korea (Project-ID: 2017013297) and BK 21 Plus project of Seoul National University.

#### REFERENCES

- [1] S. Yang, S. Yun, and T. Oda, "Molecular dynamics simulation on stability and diffusivity of hydrogen around a  $\langle 111 \rangle$  symmetric tilt grain boundary in bcc-Fe," *Fusion Eng. Des.*, vol. 131, pp. 105–110, 2018.
- [2] J. J. Quinn and K.-S. Yi, *Solid State Physics*. Berlin, Heidelberg: Springer Berlin Heidelberg, 2009.
- [3] S. Plimpton, "Fast Parallel Algorithms for Short-Range Molecular Dynamics," *J. Comput. Phys.*, 1995.
- [4] A. Ramasubramaniam, M. Itakura, and E. A. Carter, "Interatomic potentials for hydrogen in  $\alpha$ -iron based on density functional theory," *Phys. Rev. B*, vol. 79, no. 17, p. 174101, 2009.
- [5] M. Yamaguchi, J. Kameda, K.-I. Ebihara, M. Itakura, and H. Kaburaki, "Mobile effect of hydrogen on intergranular decohesion of iron: first-principles calculations," *Philos. Mag.*, vol. 92, no. 11, pp. 1349–1368, 2012.